

Short Communication

Heat transfer in an ultrasonic processing cell: Preliminary measurements

Talal Yusaf¹, David R. Buttsworth¹, and Hilton C. Deeth²

¹Faculty of Engineering and Surveying, University of Southern Queensland, Toowoomba, QLD, 4350, Australia, ²School of Land and Food, The University of Queensland, Gatton Campus, QLD, 4345, Australia

Abstract: To take full advantage of the efficiencies offered by ultrasonic processing in various applications, it can be important to minimize or utilize the ultrasonic energy that is removed from the processing volume in the form of heat. In the present work, a small volume of water is exposed to approximately 400W of ultrasonic power at 20kHz. Measurements of the convective heat transfer at the surface of the processing cell were obtained through a transient heat transfer experiment. Details of the experimental arrangement as well as the preliminary experimental heat transfer results are discussed. It was found that the overall heat losses in the present arrangement represents less than 5% of the applied ultrasonic power.

Key words: Ultrasonic, energy, heat transfer, transient heat transfer.

Introduction

The use of high-power ultrasound for various manufacturing and materials processing applications is well established. Ultrasonic processing has also been used food processing applications (Sala et al., 1995), and the particular application that motivates the present work is that of milk sterilization using ultrasonic treatments (Villamiel et al., 1999, 2000).

Experimental studies of microorganism inactivation using ultrasonic treatments have been performed over many decades and it is clear that ultrasonic treatments can damage or destroy certain microorganisms (Sala et al., 1995). However, commercial implementation of ultrasonic treatments for milk sterilization have not yet been realized for a number of reasons.

Ultrasonic treatments of microorganisms are sensitive to a wide range of parameters that have not always been thoroughly reported in the literature. Hence, apparently conflicting results are sometimes reported and replication of previously reported treatments is often difficult (Kinsloe et al., 1954; Alliger, 1978; Sala et al., 1995). Furthermore, prohibitively high power levels have sometimes been necessary to inactivate certain bacteria. Hence, the advantage of ultrasonic treatments from economic and energy perspectives is not yet clear.

The present work represents and attempts to quantify the heat transfer associated with ultrasonic processing so that: 1) future experimental results on microorganism disruption can be reported with greater clarity; and 2) the economic viability of proposed ultrasonic treatments can be accurately assessed.

Apparatus

The ultrasonic treatment apparatus consisted of a commercial ultrasonic processor (Dr. Hielscher GmbH, type: UIP500) attached to a 316 stainless steel processing cell as illustrated in Figure 1. For the bacteria inactivation experiments, the processing cell can be used in either a batch or continuous flow arrangement. For continuous flow operation, ports on the side and base of the processing cell are used. However, for the present heat transfer experiments, the cell was operated in a batch configuration with a perspex base which did not have a flow port.

The ultrasonic processor provided approximately 400W of power (at 20 kHz) to a sample of approximately 4ml of water in the processing cell. Three thermocouples (type K) were located to various points around the processing cell as illustrated in Figure 1. The most important thermocouples are the water temperature thermocouple (giving the value, T_w) and the

thermocouple located at the perspex surface in contact with the water (giving the value, T_{sp}). The thermocouple located on the lower surface of the perspex (giving the value, T_l) was used to indicate the time at which the heat transfer within the perspex departed from the assumed semi-infinite process. Signals from the thermocouples were amplified using an integrated circuit with cold junction compensation (Analogue Devices, AD595) and the temperature signals (voltages) were recorded at 20 Samples/s using an A/D card and LabView software.

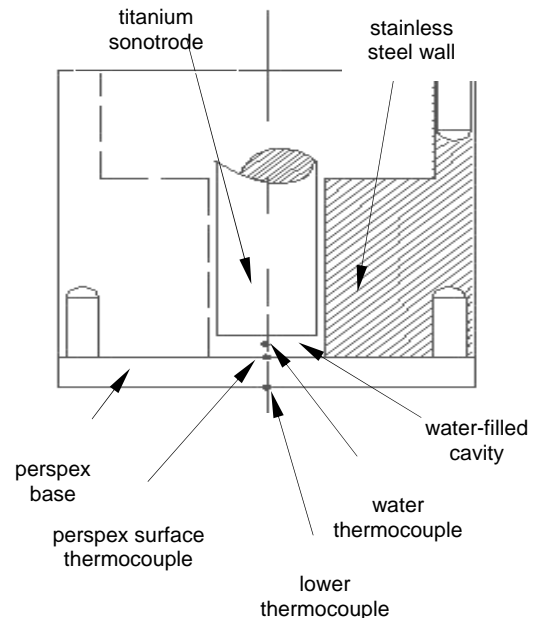


Figure 1. Illustration of the ultrasonic processing cell.

Nomenclature

- c specific heat (J/kgK)
- k conductivity (W/mK)
- h heat transfer coefficient (W/m²K)
- q heat transfer rate (W/m²)
- R radius of the heat conducting surface (m)
- s Laplace variable
- T temperature (K)
- t time after start of heat transfer (s)
- α thermal diffusivity (m²/s)
- ρ density (kg/m³)
- τ dummy variable for integration wrt time

Subscripts

- i* initial value
- l* lower surface of perspex
- s* surface heat conducting substrate
- sp* surface of perspex
- ss* surface of stainless steel
- st* surface of titanium
- w* water

Experimental Results

Measurements from the three thermocouples over a period of 5min after switching on the ultrasonic processor are presented in Figure 2. Time 0 in Figure 2 corresponds to the point at which the ultrasonic processor was switched on. The actual temperature differences relative to the initial (pre-run) level are presented in Figure 2. It is these differences in temperature that are necessary in the transient heat flux analysis (see Section 4). The initial temperatures indicated by each thermocouple were: $T_w=15^\circ\text{C}$, $T_{sp}=17^\circ\text{C}$, and $T_l=18^\circ\text{C}$.

Two relatively large disturbances appeared on the signal from the water temperature thermocouple – the first at about 15s and the second at around 140s on the time scale in Figure 2. The second of these disturbances has been removed from the signal presented in Figure 2, and hence the data appears unrealistically smooth in this region. These disturbances may be attributed to thermocouple damage from the ultrasonic treatment (causing microscopic cavitation bubbles) as during subsequent testing, the hot junction of the water thermocouple went open circuit. Alternatively, the disturbances may be an electromagnetic interference from some as yet unidentified source as they also appear on the perspex surface thermocouple signal (but with a much smaller magnitude).

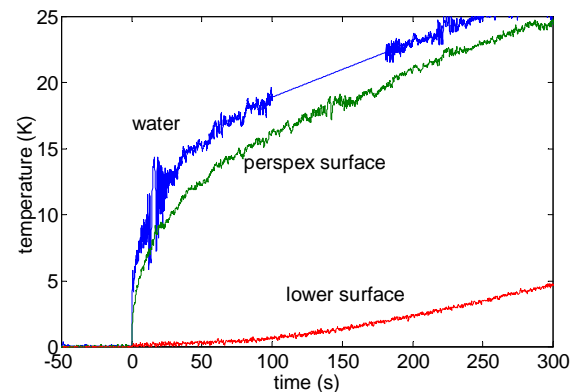


Figure 2. Temperature measurements from thermocouples.

Heat Transfer Analysis

Perspex surface

Provided the substrate into which heat is transferred can be regarded as semi infinite, the surface heat flux can be identified from measurements of surface temperature. In the case of a flat surface without any lateral conduction effects, Schultz and Jones (1973) demonstrated that the appropriate expression is

$$q = \frac{\sqrt{\rho ck}}{\sqrt{\pi}} \int_0^t \frac{dT_s}{d\tau} \frac{1}{\sqrt{(t-\tau)}} d\tau \quad (1)$$

A numerical implementation of Eq. (1) has been used to identify the heat flux to the surface of the perspex from the T_{sp} results (in Figure 2). Approximate values for the perspex thermal properties (ρ , c , and k) are presented in Table 1. Assuming the calculated value of heat flux applies across the entire perspex surface exposed to the water (an area of 531mm^2), the heat transfer to the perspex surface can be obtained as illustrated in Figure 3.

Table 1. Properties of materials used in the processing cell construction

Material	ρ (kg/m^3)	C (J/kgK)	k (W/mK)	α ($10^{-6}\text{m}^2/\text{s}$)
Perspex	1200	1450	0.2	0.11
Stainless steel	8300	470	13	3.3

Titanium	4500	520	22	9.4
----------	------	-----	----	-----

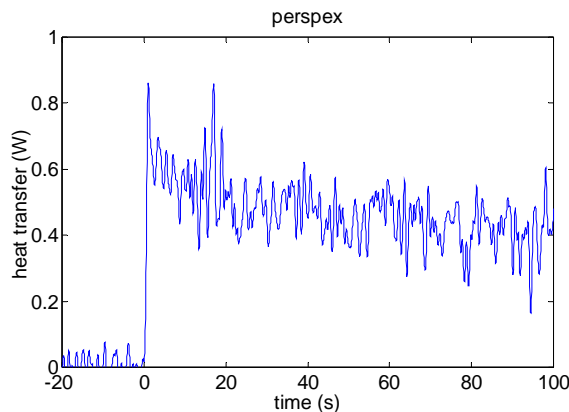


Figure 3. Heat transfer to the perspex.

From Figure 2, a measurable increase in temperature at the lower surface of the perspex is apparent approximately 1min after heating begins. This is to be expected since the thickness of the perspex was $x=12.7\text{mm}$ and the thermal diffusivity of perspex (Table 1) was $\alpha=0.11\times 10^{-6}\text{m}^2/\text{s}$, so that the heat penetration time (Schultz and Jones, 1973) is

$$t = \frac{x^2}{16\alpha} = 92\text{s} \quad (1)$$

Thus, approximately semi-infinite conditions persist for about 100s after the start of heating (the time at which the ultrasonic processor was switched on).

Assuming that the induced flow and thermal transport conditions within the processing cell remain constant during the experiment, the surface heat flux should be proportional to the difference in temperature between the water and the surface,

$$q = h(T_w - T_s) \quad (2)$$

where the constant of proportionality h , is the convective heat transfer coefficient.

The Equation (2) has been used in conjunction with the water and perspex surface temperature measurements and the perspex heat flux results from Eq. (1) to estimate the heat transfer coefficient. Results from this analysis are presented in Figure 4. Convective heat transfer coefficient data prior to the start of the

ultrasonic processor is not meaningful and has not been included in Figure 4. Likewise the data from around 15s is contaminated by the large disturbance on the water thermocouple at this time (see Section 3) and hence is also not included in Figure 4.

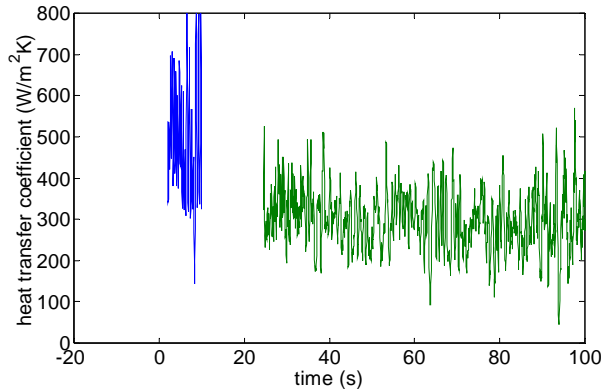


Figure 4. Heat transfer coefficient at the perspex.

From Figure 4 it is observed that the apparent heat transfer coefficient is not exactly constant, but steadily decreases from a value of approximately $500\text{W}/\text{m}^2\text{K}$ at the start of heating to about $300\text{W}/\text{m}^2\text{K}$ at a time 100s after the start of heating.

In the present experiments, the water temperature changed by around 18°C in the first 100s. The associated changes in viscosity and thermal conductivity would be around 30% and 5% respectively. Thus some variation in the heat transfer coefficient would be expected. Another effect that may contribute to the apparent variation in heat transfer coefficient is the fact that the ultrasonic processor was switched on from cold, and it may actually require a few minutes to reach a steady operating condition.

Another factor that may contribute to the apparent variation in heat transfer coefficient with time is lateral conduction. Such effects have been assumed to be negligible. However, lateral conduction is likely to be present since there will be a

heat flux-induced temperature difference between the perspex and the stainless steel.
 Stainless steel surface

In the case of the vertical stainless steel wall which is a concave cylindrical surface, a convenient (approximate) expression for the relationship between the heat flux and the measured surface temperature is (Buttsworth and Jones, 1997)

$$q = \frac{\sqrt{\rho ck}}{\sqrt{\pi}} \int_0^t \frac{dT_s}{d\tau} \frac{1}{\sqrt{(t-\tau)}} d\tau + \frac{k}{2R}(T_s - T_i) \quad (3)$$

The Laplace transformation of Eq. (3) is

$$\bar{q} = \sqrt{\rho ck} \sqrt{s} \bar{T}_s + \frac{k}{2R} \bar{T}_s \quad (4)$$

where the over line denotes the Laplace transformation. Assuming the convective heat transfer coefficient is constant, the Laplace transformation of Eq. (2) is

$$\bar{q} = h(\bar{T}_w - \bar{T}_s) \quad (5)$$

Subtracting Eq. (5) from Eq. (4) gives an expression for the surface temperature:

$$\bar{T}_s = G(s)\bar{T}_w \quad (6)$$

with the transfer function between the water temperature and the surface temperature given by

$$G(s) = \frac{h}{\sqrt{\rho ck}} \frac{1}{\sqrt{s+a}} \quad (7)$$

where

$$a = \frac{k+2Rh}{2R\sqrt{\rho ck}} \quad (8)$$

The inverse Laplace transformation of Eq. (7) is

$$g(t) = \frac{h}{\sqrt{\rho ck}} \left(\frac{1}{\sqrt{\pi t}} - ae^{a^2 t} \operatorname{erfc}(a\sqrt{t}) \right) \quad (9)$$

The surface temperature history can therefore be obtained from Eq. (6) using the convolution integral,

$$T_s = \int_0^t g(\tau) T_w(t-\tau) d\tau \quad (10)$$

No thermocouple was located on the stainless steel surface. However, the surface temperature history can be estimated using

Eq. (10) if the heat transfer coefficient on the stainless steel is assumed to be constant and equal to the heat transfer coefficient measured at the perspex surface. The constant value adopted for the convective heat transfer coefficient was $h=500\text{W/m}^2\text{K}$. The derived surface temperature history for the stainless steel is presented in Figure 5.

Having estimated the stainless steel surface temperature history (Figure 5), the surface heat flux can be calculated using Eq. (2). Heat transfer to the stainless steel as determined with this method is presented in Figure 6. As was the case with the perspex results in Figure 3, the heat flux results (expressed in W/m^2) have been scaled by the relevant surface area (approximately 1633mm^2 in this case) in Figure 6.

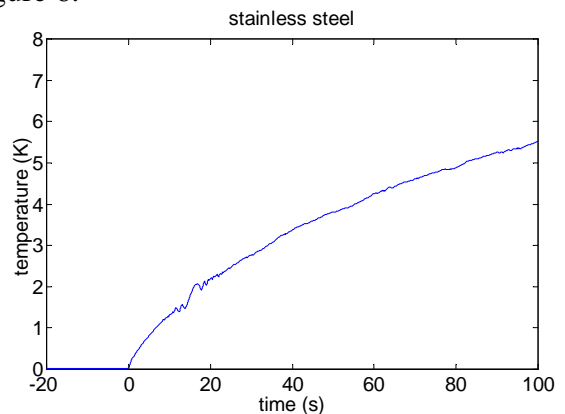


Figure 5. Surface temperature of the stainless steel.

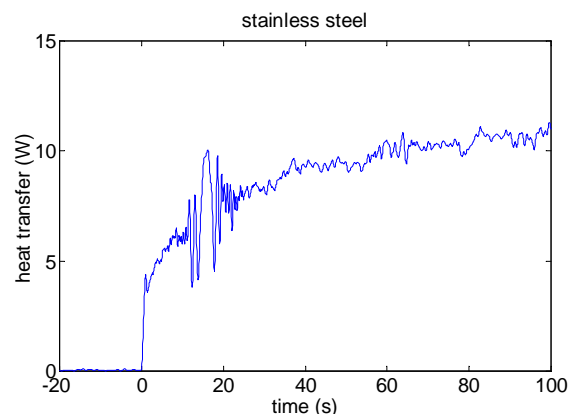


Figure 6. Heat transfer to the stainless steel.

Limitations of the above analysis include the approximate nature of Eq. (3) which produces results within 1% of the actual solution for heating times such that

$$\frac{\alpha t}{R^2} \approx 0.1$$

(Buttsworth and Jones, 1997). In the present configuration (stainless steel with a radius of 13mm), the above criterion indicates a time of 5s. This suggests that after the first few seconds of the experiment, significant errors may be introduced because of the limitations of Eq. (3).

Additional limitations arise because it has been assumed that the heat transfer coefficient on the stainless steel is the same as that on the perspex surface. Furthermore, the heat transfer coefficient is actually treated as constant, even though experimentally this is not the case (see Figure 4).

Titanium surface

Heat transfer to the titanium surface (the sonotrode tip) can be estimated using the analysis outlined in Section 4.2. Slight adjustments to the analysis of Section 4.2 need to be made to accommodate the fact that the titanium is a flat surface ($R \rightarrow \infty$) with significantly different thermal properties than the stainless steel (Table 1). When this is done, the resulting heat transfer across an area of 380mm² (the area of the sonotrode) is obtained as presented in Figure 7.

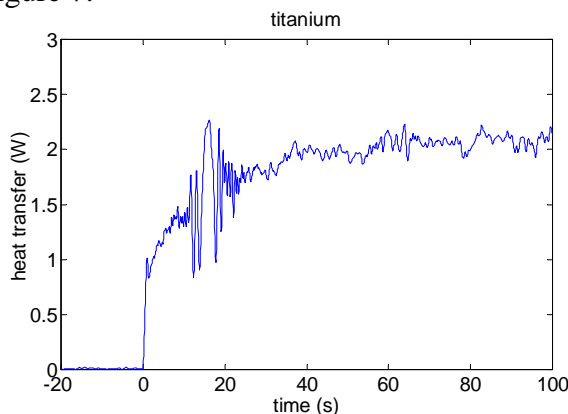


Figure 7. Heat transfer to the titanium. Discussion

Due to the transient nature of the present experiments, the heat transfer to the surfaces of the processing cell vary with time. To obtain some indication of relative magnitudes, the time 100s after the start of the ultrasonic processor is considered. At this point, the heat transfer to the perspex, stainless steel, and titanium surfaces is approximately 0.4, 11, and 2.1W respectively. Thus the combined heat transfer from the water is around 14W or about 3.5% of the applied ultrasonic power.

Summary and Conclusions

Transient one dimensional heat conduction modeling has been applied to evaluate the heat transfer to the surfaces of an ultrasonic processing cell. The processing cell was filled with water and instrumented with thermocouples. Ultrasonic power at 20kHz and approximately 400W was applied for a few minutes and temperature histories were recorded.

Estimates for the current configuration suggest that less than 5% of the applied ultrasonic power was removed from the processing volume in the form of heat. This estimated value is configuration dependent, and may be substantially larger in some applications. Such heat transfer could have a significant impact on efficiency calculations for the ultrasonic processor based on calorimetric experiments in this and related configuration.

There are a number of limitations of the present data and analysis. In particular, the heat transfer coefficient appears to vary with time. This may be a real effect as the water temperature does change with time, and the ultrasonic processor was started from cold. However, modeling deficiencies

such as the semi infinite one dimensional heat conduction assumption may also contribute to the apparent variation with time. Additional experiments will be performed in the near future using a refined procedure and more extensive instrumentation in order to improve the precision of the heat transfer measurements.

Acknowledgement

The financial support of the Dairy Research and Development Corporation and Dairy Farmers is gratefully acknowledged.

References

- Alliger, H. 1978. New methods in ultrasonic processing. American Laboratory 10:81-87.
- Buttsworth, D. R. and T. V. Jones. 1997. Radial conduction effects in transient heat transfer experiments. Aeronautical J. 101 (1005):209-212.
- Kinsloe, H., E. Ackerman and J. J. Reid. 1954. Exposure of microorganisms to measured sound fields. J. Bacteriology 68: 373-380.
- Sala, F. J., J. Burgos, S. Condon, P. Lopez and J. Raso. 1995. Effect of heat and ultrasound on microorganisms and enzymes. In: G. W. Gould (Ed.). pp. 176-204. New Methods of Food Preservation. Blackie, London.
- Schultz, D. L. and T. V. Jones. 1973. Heat transfer measurements in short-duration hypersonic facilities, Advisory Group for Aerospace Research and Development. AGARD-AG-165.
- Villamiel, M., E. H. Van Hamersveld and P. De Jong. 1999. Review: Effect of ultrasound processing on the quality of

dairy products. *Milchwissenschaft* 54: 69-73.

- Villamiel, M. and P. de Jong. 2000. Inactivation of *Pseudomonas fluorescens* and *Streptococcus thermophilus* in Trypticase Soy Broth and total bacteria in milk by continuous-flow ultrasonic treatment and conventional heating, *J. Food Eng.* 45:171-179.